Registry No. (Et_4N)[Fe(salen)(SH)], 114324-79-7; Na[Fe(salen)(EtS)], 114324-80-0; Na[Fe(salen)(*t*-BuS)], 114324-81-1; Na[Fe(salen)(Me_3SiS)], 114324-82-2; (Et_4N)[Fe(salen)(PhS)], 114324-84-4; (Et_4N)[Fe(salen)(*p*-MeC_6H_4S)], 114324-86-6; Na[Fe(salen)(2,6-$Me_2C_6H_3S$)], 114324-87-7; Na[Fe(salen)(2,4,6-$Me_3C_6H_2S$)], 114324-88-8; (Et_4N)[Fe(salen)Cl], 114324-90-2; (Et_4N)[Fe(salen)F], 114324-92-4; (Et_4N)[Fe(salen)(CN)], 114324-94-6; (Et_4N)[Fe(salen)(NCS)], 114324-96-8; (Et_4N)[Fe(salen)(OH)], 114324-98-0; Na[Fe(salen)(*p*-MeC_6H_4O)], 114324-99-1; Fe(salen)$(DMF)_2$, 114325-00-7; Fe(salen)$(py)_2$, 54477-48-4; Fe(3-*t*-Busalen)Cl, 114325-01-8; Fe(5-*t*-Busalen)Cl, 114325-02-9; Fe(5-NO_2salen)Cl, 62945-13-5; Fe(3-*t*-Busalen)(S-*p*-tol), 114325-03-0; Fe(5-*t*-Busalen)(S-*p*-tol), 114325-04-1; (Et_4N)[Fe(5-NO_2salen)(S-*p*-tol)], 114325-06-3; [Fe(3-*t*-Busalen)(S-*p*-tol)]$^-$, 114325-07-4; [Fe(5-NO_2salen)(S-*p*-tol)]$^-$, 114325-05-2; Fe(salen)(S-*p*-tol), 81276-94-0; (Et_4N)(SPh), 3193-72-4; (Et_4N)(S-*p*-tol), 76750-18-0; HS-*p*-tol, 106-45-6; HSPh, 108-98-5; Fe(salen), 14167-12-5.

Supplementary Material Available: A table of iron analyses for compounds in Table I and crystallographic data for (Et_4N)[Fe(5-NO_2salen)(S-*p*-tol)], including tabulations of positional and thermal parameters, interatomic distances and angles, and calculated hydrogen atom positions (6 pages); a table of calculated and observed structure factors (22 pages). Ordering information is given on any current masthead page.

Contribution from the Departments of Chemistry, Florida Atlantic University, Boca Raton, Florida 33431, and Indiana University-Purdue University at Indianapolis, Indianapolis, Indiana 46223

Relationship between Structural Change and Heterogeneous Electron-Transfer Rate Constant in Iron-Tetraphenylporphyrin Complexes

Diwei Feng[1a] and Franklin A. Schultz*[,1b]

Received December 11, 1987

The rate of metal-centered electrochemical reduction is reported for six high-spin iron(III)-tetraphenylporphyrin (TPP) complexes, Fe(TPP)X (X = Br^-, Cl^-, F^-, $C_6H_5O^-$, CH_3O^-, $CH_3CO_2^-$), three low-spin iron(III) complexes, Fe(TPP)X_2 (X = pyridine, imidazole, CN^-), and a manganese(III) complex, Mn(TPP)Cl, in CH_2Cl_2. Heterogeneous electron-transfer rate constants (k_s^{app}) are smaller by 0.3-1.3 orders of magnitude for high-spin Fe(TPP)X and Mn(TPP)Cl reductions compared with those for low-spin Fe(TPP)X_2 reductions. These differences result from the greater changes in molecular structure that accompany reduction of the high-spin species and correspond to increases in the inner-shell activation energy, $\Delta(\Delta G^*_{is})$, of up to 1300 cal mol^{-1}. We have quantitatively correlated relative rate constants for Fe(TPP)X and Mn(TPP)Cl reductions with porphyrin structural data using the Marcus theory. The diminished rate of Mn(TPP)Cl charge transfer derives exclusively from the large increase (0.37 Å) in metal out-of-plane displacement that accompanies reduction of Mn(TPP)Cl to [Mn(TPP)Cl]$^-$; no change occurs in the axial Mn-Cl dimension. High-spin Fe(TPP)X reductions are accompanied by increases in both the metal out-of-plane distance and axial Fe-X bond length. The latter term is the predominant contributor to $\Delta(\Delta G^*_{is})$; thus, k_s^{app} for Fe(TPP)X reduction decreases systematically as the frequency of the Fe-X vibration increases.

Introduction

Iron porphyrins are important model compounds for hemoproteins.[2,3] There is considerable interest in the electrochemistry of these complexes[4] as a guide to understanding the electron-transfer behavior of heme centers in naturally occurring systems. Electrochemical studies commonly have addressed the influence of porphyrin structure and axial ligation on half-wave potentials[5] and the stoichiometry[6] of electrode half-reactions. These relationships are reasonably well understood. The same structural features influence the kinetics of metal-centered electron-transfer reactions of porphyrins.[7-13] Generally, it is true that electron transfers involving high-spin/high-spin or high-spin/low-spin couples are slower than those involving low-spin species exclusively. However, specific factors underlying the dependence of electron transfer rate on porphyrin structure and spin state remain poorly understood.

High-spin ($S = {}^5/_2$) iron(III) porphyrins, Fe(P)X, typically are five-coordinate species with the iron atom displaced substantially out of the plane toward the axial ligand, X. Low-spin ($S = 1/2$) iron(III) porphyrins, Fe(P)X_2, are six-coordinate; the two axial ligands constrain the metal to lie essentially in the porphyrin plane. In the latter case, reduction proceeds to six-coordinate iron(II) (low spin, $S = 0$) with little structural change and a relatively rapid rate of electron transfer. The slow electron-transfer rates associated with reduction of high-spin iron(III) porphyrins generally are attributed to greater activation energy barriers arising from elongation or cleavage of the axial Fe-X bond or to movement of the Fe atom with respect to the porphyrin plane. The influence of axial ligand character on electron-transfer rate at a metal-porphyrin center has been investigated in several instances,[9,12,13] but a satisfactory correlation of these parameters has not been achieved.

(1) (a) Current address: General Research Institute for Non-ferrous Metals, Beijing, People's Republic of China. (b) To whom correspondence should be addressed at IUPUI.
(2) (a) Lever, A. B. P., Gray, H. B., Eds. *Iron-Porphyrins*; Addison-Wesley: New York, 1982; Part I. (b) *Ibid.*, Part II.
(3) Scheidt, W. R.; Reed, C. A. *Chem. Rev.* **1981**, *81*, 543.
(4) Kadish, K. M. Reference 2b, pp 161-249.
(5) (a) Walker, F. A.; Beroiz, D.; Kadish, K. M. *J. Am. Chem. Soc.* **1976**, *98*, 3484. (b) Kadish, K. M.; Morrison, M. M.; Constant, L. A.; Dickens, L.; Davis, D. G. *J. Am. Chem. Soc.* **1976**, *98*, 8387. (c) Ni, S.; Dickens, L.; Tappan, J.; Davis, D. G. *Inorg. Chem.* **1978**, *17*, 228. (d) Sugimoto, H.; Ueda, N.; Mori, M. *Bull. Chem. Soc. Jpn.* **1982**, *55*, 3468.
(6) (a) Truxillo, L. A.; Davis, D. G. *Anal. Chem.* **1975**, *47*, 2260. (b) Bottomley, L. A.; Kadish, K. M. *Inorg. Chem.* **1981**, *20*, 1348. (c) Kadish, K. M.; Bottomley, L. A. *Inorg. Chem.* **1980**, *19*, 832. (d) Kadish, K. M.; Rhodes, R. K. *Inorg. Chem.* **1983**, *22*, 1090.
(7) Kadish, K. M.; Davis, D. G. *Ann. N.Y. Acad. Sci.* **1973**, *204*, 495.
(8) Martin, R. F.; Davis, D. G. *Biochemistry* **1968**, *7*, 3096.
(9) Constant, L. A.; Davis, D. G. *J. Electroanal. Chem. Interfacial Electrochem.* **1976**, *74*, 85.
(10) Kadish, K. M.; Larson, G. *Bioinorg. Chem.* **1977**, *7*, 95.
(11) Kadish, K. M.; Sweetland, M.; Cheng, J. S. *Inorg. Chem.* **1978**, *17*, 2795.
(12) Richard, M. J.; Shaffer, C. D.; Evilia, R. F. *Electrochim. Acta* **1982**, *27*, 979.
(13) Kadish, K. M.; Su, C. H. *J. Am. Chem. Soc.* **1983**, *105*, 177.

0020-1669/88/1327-2144$01.50/0

Table I. Cyclic Voltammetric Data for Determination of Heterogeneous Electron-Transfer Rate Constants

Fe(TPP)(OPh)[a]			Fe(TPP)Cl[b]		
v, V s^{-1}	ΔE_p, mV	10^2k_s, cm s^{-1}	v, V s^{-1}	ΔE_p, mV	10^2k_s, cm s^{-1}
0.019	68	1.2	0.036	80	6.8
0.038	75	0.9	0.09	90	7.0
0.095	80	1.1	0.18	100	7.3
0.19	85	1.2	1.8	170	6.6
0.26	90	1.2			6.9 ± 0.4
0.53	110	0.9			
1.3	130	1.0			
		av 1.1 ± 0.1			

[a] 0.5 mM Fe(TPP)(OPh) + 0.1 M (TBA)ClO_4/CH_2Cl_2. [b] 0.5 mM Fe(TPP)Cl + 0.01 M (TEA)Cl + 0.1 M (TBA)ClO_4/CH_2Cl_2.

In this paper we present the results of an investigation in which the rate of metal-centered reduction is measured electrochemically for six high-spin iron(III)–tetraphenylporphyrin (TPP) complexes, Fe(TPP)X, three low-spin iron(III) complexes, Fe(TPP)X_2, an admixed intermediate-spin complex, Fe(TPP)ClO_4, and a manganese(III) complex, Mn(TPP)Cl. We have used the Marcus theory[14] to correlate these rates with changes in porphyrin structure accompanying the electrode reactions. These changes are capable of explaining in both direction and magnitude the differences in electron-transfer rates observed between high- and low-spin metalloporphyrin species.

Experimental Section

Materials. Fe(TPP)Cl was purchased from Aldrich Chemical Co. Fe(TPP)Br,[6a] Fe(TPP)F,[6a] Fe(TPP)(OAc),[6a] and Fe(TPP)ClO_4[15] were synthesized from [Fe(TPP)]$_2$O and the corresponding acid according to the literature methods cited. Fe(TPP)(OMe) was prepared from Fe(TPP)Cl by the method of Kobayashi.[16] Fe(TPP)(OPh) was prepared by metathesis of Fe(TPP)(OAc) with phenol as described by Sugimoto.[5d] Mn(TPP)Cl was prepared from TPP and $MnCl_2$ as described by Adler.[17] The identity of the porphyrin complexes was confirmed by their visible spectra, which agreed in all cases with literature reports. Tetra-*n*-butylammonium perchlorate ((TBA)ClO_4, Strem Chemical Co.), tetraethylammonium chloride ((TEA)Cl, Eastman Kodak), tetra-*n*-butylammonium bromide ((TBA)Br, Aldrich), and tetra-*n*-butylammonium tetrafluoroborate ((TBA)BF_4, Southwestern Analytical Chemicals) supporting electrolytes were stored over silica gel desiccant but otherwise used as received. The solvents CH_2Cl_2, CH_3OH, and CH_3CN were spectroquality materials from Aldrich or Burdick & Jackson and were treated with 4-Å molecular sieves before use.

Methods. All cyclic voltammetry experiments were carried out in 0.1 M (TBA)ClO_4/CH_2Cl_2 except as noted. The working electrode was a 0.02-cm^2 Pt disk (Bioanalytical Systems) that was polished with 0.05-μm alumina (Buehler, Ltd.) on a microcloth before each use. The auxiliary electrode was a Pt wire. The reference electrode was a nonaqueous Ag/0.1 M $AgNO_3$ electrode (in CH_3CN). Half-wave potentials are reported with respect to this electrode without correction for liquid-junction potential. An $E_{1/2}$ of +0.10 V vs this reference was measured for ferrocene oxidation in 0.1 M (TBA)ClO_4/CH_2Cl_2. Cyclic voltammetric experiments were conducted with an EG&G PAR 173/179 potentiostat using iR compensation. A Hewlett Packard 3300A function generator served as a waveform generator. Voltammograms were recorded on a Hewlett Packard 7015B X-Y recorder at sweep rates below 0.3 V s^{-1} and on a Tektronix RM564 storage oscilloscope at sweep rates above 0.3 V s^{-1}. All measurements were carried out under an argon atmosphere at an ambient temperature of 23 ± 1 °C. Values of the apparent heterogeneous electron-transfer rate constant, k_s^{app}, were obtained by the procedure of Nicholson[18] using peak potential separations of 60–210 mV. Diffusion coefficients were calculated from cyclic voltammetric wave heights for one-electron reduction of the complexes. The fidelity of the measurement system was checked by measuring k_s^{app} for ferrocene oxidation in 0.1 M (TBA)BF_4/CH_3CN. A value of 0.19 cm s^{-1} was obtained, in good agreement with the result of 0.22 cm s^{-1} of Sharp et al.[19] This result is smaller than values more recently reported for ferrocene oxidation ($k_s \simeq 2$ cm s^{-1})[20] and may reflect some residual uncompensated solution resistance in our measurements. However, the k_s^{app} values we measure for metalloporphyrin reduction (i) are 10–100 times smaller than the value measured for ferrocene oxidation, (ii) agree with literature values 7–13 when such comparisons are possible, and (iii) exhibit variations with molecular structure (Table III), which they would not do if iR drop were controlling ΔE_p values. Thus, we conclude that our k_s^{app} values are not distorted by uncompensated solution resistance.

Typical data illustrating the determination of k_s^{app} are presented in Table I. Experimental conditions under which k_s^{app} measurements were made are given in Table II.

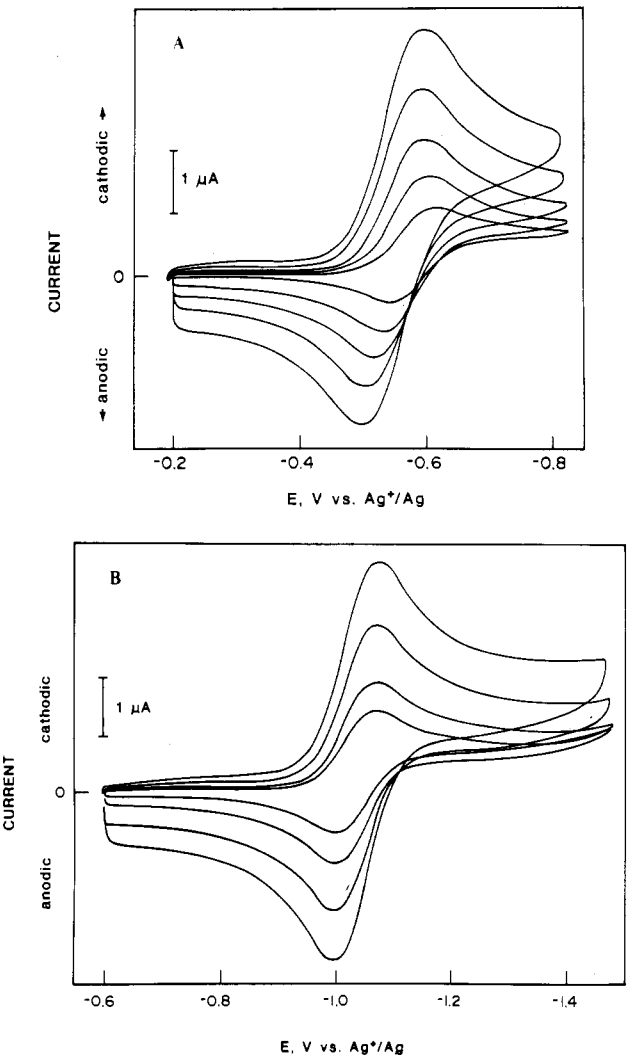

Figure 1. Cyclic voltammetric traces for reduction of (A) 0.5 mM Fe(TPP)Br in 0.1 M (TBA)Br/CH_2Cl_2 and (B) 0.5 mM Fe(TPP)(OPh) in 0.1 M (TBA)ClO_4/CH_2Cl_2. Voltammetric sweep rates from bottom to top: (A) 12, 30, 60, 120, 240 mV s^{-1}; (B) 19, 38, 95, 190 mV s^{-1}.

Results and Discussion

The five-coordinate iron(III) porphyrins examined in this work undergo metal-centered reduction without loss of axial ligand. Electrode reaction mechanism studies[6b,d,21] have shown that when relatively weak-field axial ligands (Cl^-,Br^-) or strongly coordinating solvents (DMF, DMSO) are employed, axial ligand dissociation may be coupled to the electron-transfer reaction as a chemical

(14) (a) Marcus, R. A. *Annu. Rev. Phys. Chem.* **1964**, *15*, 155. (b) Marcus, R. A. *Faraday Discuss. Chem. Soc.* **1982**, *72*, 7. (c) Marcus, R. A. *J. Chem. Phys.* **1965**, *43*, 679. (d) Sutin, N. *Acc. Chem. Res.* **1982**, *15*, 275. (e) Sutin, N. *Prog. Inorg. Chem.* **1983**, *30*, 441.
(15) Dolphin, D. H.; Sams, J. R.; Tsin, T. B. *Inorg. Chem.* **1977**, *16*, 711.
(16) Kobayashi, H.; Higuchi, T.; Kaizu, Y.; Osada, H.; Aoki, M. *Bull. Chem. Soc. Jpn* **1975**, *48*, 3137.
(17) Adler, A. D.; Longo, F. R.; Kampas, F.; Kim, J. *J. Inorg. Nucl. Chem.* **1970**, *32*, 2443.
(18) Nicholson, R. S. *Anal. Chem.* **1965**, *37*, 1351.
(19) Sharp, M.; Petersson, M.; Edstrom, K. *J. Electroanal. Chem. Interfacial Electrochem.* **1980**, *109*, 271.
(20) (a) Gennett, T.; Milner, D. F.; Weaver, M. J. *J. Phys. Chem.* **1985**, *89*, 2787. (b) Gennett, T.; Weaver, M. J. *J. Electroanal. Chem. Interfacial Electrochem.* **1985**, *186*, 179.
(21) (a) Lexa, D.; Rentien, P.; Saveant, J. M.; Xu, F. *J. Electroanal. Chem. Interfacial Electrochem.* **1985**, *191*, 253. (b) Bond, A. M.; Sweigart, D. A. *Inorg. Chim. Acta* **1986**, *123*, 167.

Table II. Experimental Conditions for k_s^{app} Measurements

complex	solution composition	sweep rate range, V s^{-1}	ΔE_p range, mV
Fe(TPP)OPh	(0.5 mM Fe(TPP)OPh + 0.1 M (TBA)ClO_4)/CH_2Cl_2	0.019–1.3	68–130
Fe(TPP)Br	(0.5 mM Fe(TPP)Br + 0.1 M (TBA)Br)/CH_2Cl_2	0.030–6.5	72–185
Fe(TPP)Cl	(0.5 mM Fe(TPP)Cl + 0.01 M (TEA)Cl + 0.1 M (TBA)ClO_4)/CH_2Cl_2	0.036–1.8	80–170
Fe(TPP)F	(0.5 mM Fe(TPP)F + 0.1 M (TBA)ClO_4)/CH_2Cl_2	0.011–0.22	85–160
Fe(TPP)OAc	(0.5 mM Fe(TPP)OAc + 0.1 M (TBA)ClO_4)/CH_2Cl_2	0.017–0.34	105–205
Fe(TPP)OMe	(0.5 mM Fe(TPP)OMe + 0.1 M (TBA)ClO_4)/CH_2Cl_2	0.032–0.09	135–180
Mn(TPP)Cl	(0.5 mM Mn(TPP)Cl + 0.1 M (TBA)ClO_4/CH_2Cl_2	0.016–0.16	100–180
Fe(TPP)ClO_4	(0.5 mM Fe(TPP)ClO_4 + 0.1 M (TBA)ClO_4)/CH_2Cl_2	3.6–9	130–170
$Fe(TPP)(py)_2^+$	(0.5 mM Fe(TPP)ClO_4 + 1 M pyridine + 0.1 M (TBA)ClO_4)/CH_2Cl_2	1.8–18	100–215
$Fe(TPP)(Im)_2^+$	(0.5 mM Fe(TPP)Cl + 1 M imidazole + 0.1 M (TBA)ClO_4)/CH_2Cl_2	4–20	125–200
$Fe(TPP)(CN)_2^-$	(0.5 mM Fe(TPP)$(H_2O)_2ClO_4$ + satd KCN)/CH_3OH	0.18–50	60–160

step. This would distort the measurement of k_s^{app}. To prevent this from occurring, reductions of Fe(TPP)Cl and Fe(TPP)Br were carried out in the presence of excess (TEA)Cl and (TBA)Br, respectively. Such dissociation was not anticipated for the stronger axial ligands (F^-, PhO^-, AcO^-, and MeO^-); thus, no excess counterion was added in these cases. Axial ligand dissociation is indicated by the presence of separate waves for Fe(TPP) and $Fe(TPP)X^-$ oxidations (the former occurring at a more positive potential) on the anodic sweep of a cyclic voltammetry experiment.[6,21] We did not observe this behavior for any of the complexes studied. As examples, parts A and B of Figure 1 illustrate the reductions of Fe(TPP)Br in the presence of excess Br^- and of Fe(TPP)(OPh), respectively. In each case, a chemically reversible voltammetric trace is observed and no wave for Fe(TPP) oxidation is detected on the positive sweep. Therefore, we conclude that the five-coordinate porphyrins undergo reduction according to

$$M(TPP)X + e^- \rightleftharpoons M(TPP)X^- \quad (1)$$

Six-coordinate iron(III) complexes also were examined in the presence of a large excess of axial ligand; under these conditions they undergo the electrode reaction

$$Fe(TPP)X_2^n + e^- \rightleftharpoons Fe(TPP)X_2^{n-1} \quad (2)$$

$$n = +1 \text{ for X = py, Im; } n = -1 \text{ for X = } CN^-$$

Table III contains values of k_s^{app} for metal-centered reduction of the 11 metalloporphyrin complexes. The metal atom spin states, half-wave potentials, and structural and spectroscopic data for some of the complexes are included. Where comparisons with literature results are possible,[7-13] our values of k_s^{app} are in good agreement with such data. One exception is [Fe(protoporphyrin)$(CN)_2$]$^-$, for which Martin and Davis[8] measured k_s^{app} = 4 cm s^{-1} in a 50:50 ethanol:water mixture by a coulostatic technique. Inexplicably, this result is greater by about 2 orders of magnitude than the electron-transfer rates of the six-coordinate iron(III)–TPP complexes.

The k_s^{app} values can be divided into three groups. High-spin/high-spin reductions cover the range 0.001–0.01 cm s^{-1}. Low-spin/low-spin reductions fall within the limits 0.02 ± 0.01 cm s^{-1}. The result for the single intermediate-spin complex, Fe(TPP)ClO_4, is 0.013 cm s^{-1}.

Within the series of high-spin/high-spin reductions, we sought to establish a relationship between k_s^{app} and the strength of the axial Fe–X bond. The effect of this structural parameter on electron-transfer rate is described by the Marcus theory applied to electrode reactions:[14c]

$$k_s^{app} = A \exp^{-\Delta G^*/RT} \quad (3)$$

A is the preexponential factor and ΔG^* is the total activation energy, which is the sum of barriers for the inner- and outer-shell reorganization processes, i.e., $\Delta G^* = \Delta G^*_{is} + \Delta G^*_{os}$. If stretching of the Fe–X bond represents part of the activational requirement for electron transfer, its contribution to ΔG^* may be expressed through the inner-shell reorganization term

$$\Delta G^*_{is} = \frac{1}{2}\sum f_i\left(\frac{\Delta a}{2}\right)^2 \quad (4)$$

Table III. Half-Wave Potential, Heterogeneous Electron-Transfer Rate Constant, Spin State, Metal Atom Out-Of-Plane Distance, and Metal Atom–Axial Ligand Vibrational Frequency for Five- and Six-Coordinate Metalloporphyrin Complexes

complex	$E_{1/2}$,[a] V vs Ag/0.1 M $AgNO_3$	$10^3 k_3^{app}$,[a] cm s^{-1}	spin state[b]	Fe–Ct_N,[b] Å	ν_{M-X}, cm^{-1}
Fe(TPP)OPh	−1.04	11 ± 1	HS		
Fe(TPP)Br	−0.58	10 ± 2	HS	0.49	270[f]
Fe(TPP)Cl	−0.72	6.9 ± 0.4	HS	0.39	357[f]
Fe(TPP)F	−0.94	2.4 ± 0.3	HS	0.47	606[f]
Fe(TPP)OAc	−0.79	1.8 ± 0.4	HS	0.49[c]	530[c]
Fe(TPP)OMe	−1.19	1.1 ± 0.1	HS	0.48[d]	540[g]
Mn(TPP)Cl	−0.72	2.4 ± 0.4	HS	0.27[e]	
Fe(TPP)ClO4	−0.27	13 ± 1	IS	0.28	
$Fe(TPP)(py)_2^+$	−0.34	20 ± 3	LS		
$Fe(TPP)(Im)_2^+$	−0.63	16 ± 2	LS	0.009	
$Fe(TPP)(CN)_2^-$	−0.89	31 ± 4	LS	0.00	

[a] Experimental conditions as noted in Table II. [b] Reference 2a, Chapter 2. [c] Oumous, H.; Lecomte, C.; Protas, J.; Cocolios, P.; Guilard, R. *Polyhedron* **1984**, *6*, 651. [d] Lecomte, C.; Chadwick, D.; Coppens, P.; Stevens, E. D. *Inorg. Chem.* **1983**, *22*, 2982. [e] Reference 29. [f] Reference 33a. [g] ν_{Fe-O} for methoxyiron(III) deuteroporphyrin IX dimethyl ester: Sadasivan, N.; Eberspaecher, H. I.; Fuchsman, W. H.; Caughey, W. S. *Biochemistry* **1969**, *8*, 534.

where f_i is the force constant of the Fe–X bond and Δa is the change in the Fe–X bond distance. Since

$$f_i = 4\pi^2\mu c^2\nu_i^2 \quad (5)$$

where μ is reduced mass, c is the speed of light, and ν_i is the stretching frequency of the Fe–X bond, a linear relationship between $-\ln k_s^{app}$ and ν_i^2 is expected if A, ΔG^*_{os}, and other factors contributing to ΔG^*_{is} remain approximately constant. Indeed, a proportionality between ΔG^*_{is} and ν_i^2 has been demonstrated[22] for the electroreduction of alkyl halides, in which stretching of the C–X bond is presumed to constitute the principal nuclear barrier to electron transfer.

Figure 2 shows the correlation between $-\ln k_s^{app}$ and $\mu\nu_i^2$ for reduction of five Fe(TPP)X complexes. The electron-transfer rate constant decreases as the donor strength of the axial ligand increases. This trend is in the direction expected if Fe–X bond stretching were to contribute to the inner-shell activation barrier for metal-centered electron transfer to high-spin Fe(III) porphyrins. The range of k_s^{app} values plotted in Figure 2 corresponds to a difference of 1300 cal/mol in activation energy between Fe(TPP)Br and Fe(TPP)OMe. In constructing this plot, we have assumed that Δa is constant. From the slope of the line in Figure 2 ($\pi^2c^2(\Delta a)^2/2RT = 3.4 \times 10^{-7}$ mol cm^2 g^{-1}) we calculate Δa = 0.14 Å. There are no structural data for Fe(III) and Fe(II) porphyrins having exactly the same porphyrin and axial ligands with which to compare this value. However, data for three $Fe^{III/II}$ pairs with very similar porphyrin and axial ligand components are collected in Table IV. These data indicate that some dif-

(22) (a) Andrieux, C. P.; Gallardo, I.; Saveant, J. M.; Su, K. B. *J. Am. Chem. Soc.* **1986**, *108*, 638. (b) Andrieux, C. P.; Saveant, J. M.; Su, K. B. *J. Phys. Chem.* **1986**, *90*, 3815.

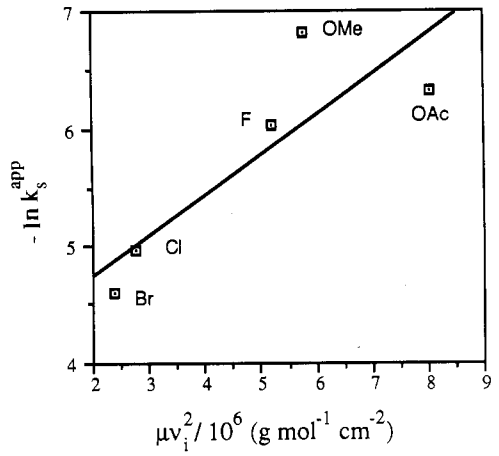

Figure 2. Correlation of heterogeneous charge-transfer rate constant with Fe–X stretching frequency for metal-centered reduction of Fe(TPP)X complexes. The total mass of the OMe and OAc fragments was used to calculate μ for Fe–OMe and Fe–OAc.

Table IV. Comparative Structural Data for M^{3+} and M^{2+} Metalloporphyrin Complexes

complex[a]	spin state	M–Ct_N,[b] Å	M–N, Å	M–X, Å	ref
Fe^{III}(MPIXDME)(OCH_3)	HS	0.49	2.073	1.842	24
Fe^{II}(porphyrin)[c]	HS	0.70	2.140	1.90	23
Δ(Fe(III)–Fe(II))		0.21	0.067	0.06	
Fe^{III}(MPIXDME)(OCH_3)	HS	0.49	2.073	1.842	24
$[Fe^{II}(TP_{piv}P)(OC_6H_5)]^-$	HS	0.57	2.114	1.937	25
Δ(Fe(III)–Fe(II))		0.08	0.041	0.097	
Fe^{III}(PPIXDME)($SC_6H_4NO_2$)	HS	0.43	2.064	2.324	26
$[Fe^{II}(TPP)(SC_2H_5)]^-$	HS	0.52	2.096	2.360	27
Δ(Fe(III)–Fe(II))		0.09	0.032	0.036	
$[Fe^{III}(TPP)(Im)_2]^+$	LS	0.009	1.989	1.991	28
$[Fe^{II}(TPP)(1\text{-MeIm})_2]$[d]	LS	0.005	2.002	2.014	3
Δ(Fe(III)–Fe(II))		0.004	0.013	0.023	
Mn^{III}(TPP)Cl	HS	0.27	2.009	2.360	29
$[Mn^{II}(TPP)Cl]^-$	HS	0.64	2.160	2.364	30
Δ(Mn(III)–Mn(II))		0.37	0.151	0.004	

[a] Abbreviations: MPIXDME, mesoporphyrin IX dimethyl ester; $TP_{piv}P$, pivalamide "picket fence" porphyrin; PPIXDME, protoporphyrin IX dimethyl ester; TPP, tetraphenylporphyrin. [b] Distance from the metal to the center of the best plane of the four porphyrin nitrogens. [c] Estimated value for Fe(II) porphyrins. [d] Representative values for compounds of this class.

ference in Δa may exist as the axial ligand is varied but that an extension of ~0.05–0.1 Å in the Fe–X distance may be expected upon reduction of high-spin Fe(III) to high-spin Fe(II). This result agrees reasonably well with the plot in Figure 2.

It is necessary to consider other contributions to the inner-shell activation barrier for Fe(TPP)X reduction. Table IV shows that significant differences in the Fe–Ct_N and Fe–N distances exist between Fe(III) and Fe(II). These differences correspond to increased displacement of the iron atom above the porphyrin plane and to lengthening of the Fe–N bonds upon metal-centered reduction. These features, which originally were predicted by Hoard,[23] result from the change in electronic configuration that

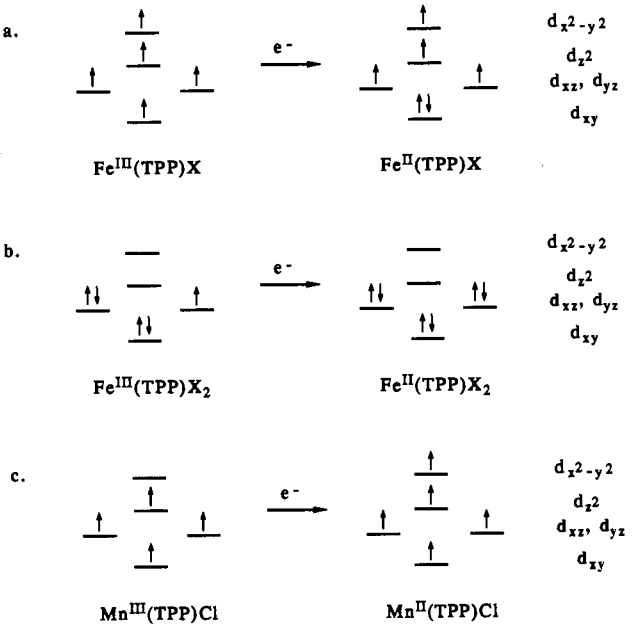

Figure 3. Changes in electronic configuration accompanying M(III)/M(II) reductions: (a) high-spin Fe(TPP)X; (b) low-spin Fe(TPP)X_2; (c) Mn(TPP)Cl.

occurs upon reduction of Fe(III) to Fe(II) in a high-spin porphyrin environment. As depicted in Figure 3a, this reduction adds a second electron to the d_{xy} orbital. When doubly occupied, this orbital corresponds to the "phantom ligand" described by Hoard,[23] which interacts repulsively with bonds to the porphyrin nitrogen atoms and results in increases in the Fe–Ct_N and Fe–N distances.[31] Corresponding changes do not occur upon reduction of six-coordinate, low-spin Fe(III) porphyrins. Here, the d_{yz} orbital that becomes doubly occupied upon electrochemical reduction is effectively nonbonding with respect to both porphyrin nitrogen and axial ligands (Figure 3b). Thus, as confirmed by the structural data in Table IV, there are only small differences in Fe–Ct_N, Fe–N, and Fe–X distances between the Fe(III) and Fe(II) oxidation states for this class of compounds. We conclude that these different extents of structural change are responsible for the difference in electron-transfer rates between five-coordinate high-spin iron(III) porphyrins and six-coordinate low-spin Fe(III) porphyrins.

The inner-shell activation energy barrier for high-spin iron(III) porphyrin reduction should contain contributions from both Fe–X bond lengthening and Fe–porphyrin out-of-plane displacement. We will present approximate calculations of these quantities from the iron–porphyrin structural data in Table IV. However, we first wish to verify the applicability of such calculations to molecules of this type by examining a redox couple for which the structures of both the reduced and oxidized species are known. The Mn–tetraphenylporphyrin complexes Mn^{III}(TPP)Cl[29] and $[Mn^{II}$(TPP)$Cl^-]$[30] fulfill this requirement. Structural data are reported in Table IV, and the electrochemical rate constant for Mn(TPP)Cl reduction (eq 1, M = Mn, X = Cl) is reported in Table III. Here, the change from d^4 Mn(III) to d^5 Mn(II) results in occupation of the $d_{x^2-y^2}$ orbital (Figure 3c), which is strongly antibonding with respect to the metal–porphyrin bonds. Consequently, there are large changes in the Mn–N (0.151 Å) and Mn–Ct_N distances (0.37 Å), but virtually none in the Mn–Cl distance (0.001 Å). Thus, the inner-shell activation barrier for Mn(TPP)Cl reduction should consist entirely of the metal out-of-plane displacement term. This energy is represented by the extension of four Mn–N bonds by 0.15 Å at a frequency ν_{Mn-N} = 275 cm^{-1}.[32,33] The Mn–Cl

(23) Hoard, J. L. *Science (Washington, D.C.)* **1971**, *174*, 1295.
(24) Hoard, J. L.; Hamor, M. J.; Hamor, T. A.; Caughey, W. S. *J. Am. Chem. Soc.* **1965**, *87*, 2312.
(25) Nasri, H.; Fischer, J.; Weiss, R.; Bill, E.; Trautwein, A. *J. Am. Chem. Soc.* **1987**, *109*, 2549.
(26) Tang, S. C.; Koch, S.; Papaefthymiou, G. C.; Foner, S.; Frankel, R. B.; Ibers, J. A.; Holm, R. H. *J. Am. Chem. Soc.* **1976**, *98*, 2414.
(27) Caron, C.; Mitschler, A.; Riviere, G.; Ricard, L.; Schappacher, M.; Weiss, R. *J. Am. Chem. Soc.* **1979**, *101*, 7401.
(28) Collins, D. M.; Countryman, R.; Hoard, J. L. *J. Am. Chem. Soc.* **1972**, *94*, 2066.
(29) Tulinsky, A.; Chen, B. M. L. *J. Am. Chem. Soc.* **1977**, *99*, 3647.
(30) VanAtta, R. B.; Strouse, C. E.; Hanson, L. K.; Valentine, J. S. *J. Am. Chem. Soc.* **1987**, *109*, 1425.

(31) Hoard suggested that little or no change in axial Fe–X distance should accompany high-spin Fe(III) to high-spin Fe(II) reduction. However, the structural data in Table II and our electrochemical results suggest that such a change does occur, probably as a result of the increased radius of Fe(II) compared to that of Fe(III).[3]

group is assumed to move as a single unit of atomic mass 90.5. These values result in a force constant of 0.54×10^5 dyn cm^{-1} for the Mn–N bond, from which a value of $\Delta G^{\ddagger}_{is} = 900$ cal mol^{-1} is calculated.

The rate constant for electrochemical reduction of Mn(TPP)Cl is $k_s^{app} = 2.4 \times 10^{-3}$ cm s^{-1} (Table III). If it is assumed that the decrease in the magnitude of this parameter relative to that for low-spin Fe(III) porphyrin reduction ($k_s^{app} \simeq 0.02$ cm s^{-1}) is due entirely to metal out-of-plane displacement, then the accuracy of the calculated activation energy can be assessed from the experimentally measured rate constant ratio via eq 6, where

$$(k_s^{app})_{MPX}/(k_s^{app})_{MPX_2} = e^{-\Delta(\Delta G^{\ddagger}_{is})/RT} \quad (6)$$

$\Delta(\Delta G^{\ddagger}_{is})$ is the additional inner-shell activation energy associated with high-spin reduction. The experimental result is $(k_s^{app})_{MPX}/(k_s^{app})_{MPX_2} = 0.12$; $\Delta(\Delta G^{\ddagger}_{is}) = 900$ cal mol^{-1} predicts a rate constant ratio of 0.22. Thus, the difference in rate constants is largely accounted for by the increment in metal out-of-plane distance that accompanies Mn(TPP)Cl reduction.

We now return to the high-spin Fe(TPP)X reductions. The incremental inner-shell activation barriers for this process are the sum of energies for out-of-plane displacement, $(\Delta G^{\ddagger}_{is})_{oop}$, and extension of the axial Fe–X bond, $(\Delta G^{\ddagger}_{is})_{ax}$.

$$\Delta(\Delta G^{\ddagger}_{is}) = (\Delta G^{\ddagger}_{is})_{oop} + (\Delta G^{\ddagger}_{is})_{ax} \quad (7)$$

We assume that $(\Delta G^{\ddagger}_{is})_{oop}$ is the same for all reductions of this type and, by reference to Table IV, is represented by the extension of four Fe–N bonds by 0.05 Å with $\nu_{Fe-N} = 275$ cm^{-1}. A common mass of 100 is assumed for the Fe–X unit. The calculated value is $(\Delta G^{\ddagger}_{is})_{oop} = 100$ cal mol^{-1}. A smaller magnitude relative to Mn(TPP)Cl reduction is expected from the smaller metal atom displacement (0.05 Å, ΔFe–N vs 0.15 Å, ΔM–N).

The largest and smallest rate constants for Fe(TPP)X reduction are represented by the values for Fe(TPP)Br and Fe(TPP)OMe. We therefore calculate $(\Delta G^{\ddagger}_{is})_{ax}$ for these two species to indicate the range of inner-shell energies that can be assigned to Fe–X bond extension. We assume Δa to be constant and equal to 0.14 Å and take $\mu = 33$ and $\nu_{Fe-X} = 270$ cm^{-1} for Fe(TPP)Br and $\mu = 20$ and $\nu_{Fe-X} = 540$ cm^{-1} for Fe(TPP)OMe. The results are $(\Delta G^{\ddagger}_{is})_{ax} = 500$ cal mol^{-1} for Fe(TPP)Br and 1210 cal mol^{-1} for Fe(TPP)OMe; the total activation energy differences (eq 7) are 600 and 1310 cal mol^{-1}, respectively. If these numbers are substituted for $\Delta(\Delta G^{\ddagger}_{is})$ in eq 6, it is predicted that the rate constants for high-spin iron(III) porphyrin reduction $[(k_s^{app})_{MPX}]$ will range from 0.11 to 0.36 times the value for low-spin iron(III) porphyrin reduction $[(k_s^{app})_{MPX_2} \simeq 0.02$ cm s$^{-1}]$. The experimentally measured rate constant ratios range from 0.06 to 0.5 (Table III). The Marcus theory therefore accounts for the slow, axial ligand dependent electron-transfer rate of high-spin Fe(III) porphyrins although the range of values predicted is not as large as is observed experimentally.

We have shown that the difference in heterogeneous electron-transfer rate constants between high- and low-spin M(III)–porphyrin complexes can be accounted for by the greater changes in nuclear coordinates that accompany the charge-transfer reactions of the former. The nuclear reorganization may consist primarily of metal out-of-plane displacement, as is the case for Mn(TPP)Cl reduction, or may be a sum of metal out-of-plane displacement and elongation of the axial ligand bond (with this factor predominanting), as for Fe(TPP)X reduction. These factors cause the rate constant for reduction of high-spin metalloporphyrin species to be 0.3–1.3 orders of magnitude smaller than those of low-spin complexes. The difference in electron-transfer rate constants between high- and low-spin metalloporphyrin complexes appears to extend to homogeneous solution reactions as well.[34] Electron-self-exchange rate constants of 10^3–10^6 M^{-1} s^{-1} have been measured for five-coordinate high-spin porphyrins and of 10^7–8×10^{10} M^{-1} s^{-1} for six-coordinate low-spin porphyrins.[35] We expect that a similar structural explanation is responsible for the lower rates exhibited by the high-spin species.

Table V. Comparison of Measured and Calculated Heterogeneous Rate Constants for Metalloporphyrin Charge-Transfer Reactions

reacn	k_{ex}^{homo},[a] M^{-1} s^{-1}	$(k_s^{app})_{measd}$, cm s^{-1}	$(k_s^{app})_{calcd}$, cm s^{-1}
HS metal-centered	10^3–10^6	1×10^{-3}–1×10^{-2}	1×10^0–3×10
LS metal-centered	10^7–8×10^{10}	1×10^{-2}–1×10^{-1}	1×10^2–9×10^3
porphyrin ring	10^8 [b]	1×10^{-2}–1×10^{-1}	3×10^2

[a] From ref 35. [b] Assumed equal to the value for electron self-exchange in chlorophylls: Closs, G. L.; Sitzmann, E. V. *J. Am. Chem. Soc.* **1981**, *103*, 3217.

Finally, it is of interest to compare heterogeneous rate constants for high-spin metal-centered, low-spin metal-centered, and porphyrin-ring-centered[37] charge-transfer reactions with values predicted from the corresponding homogeneous self-exchange reactions using the Marcus relation.[14c]

$$(k_s^{app})_{calcd} = Z_{het}\left(\frac{k_{ex}^{homo}}{Z_{homo}}\right)^{1/2} \quad (8)$$

Comparisons based on eq 8 with $Z_{het} = 10^4$ cm s^{-1} and $Z_{homo} = 10^{11}$ M^{-1} s^{-1} are summarized in Table V and show that $(k_s^{app})_{calcd}$ is larger than $(k_s^{app})_{measd}$ by 3–5 orders of magnitude. Reasons for differences between derived and measured rate constants of this type have been discussed.[38] However, the case of slow heterogeneous electron transfer to metalloporphyrin species appears to merit special consideration. For example, when $(k_s^{app})_{calcd}$ is derived from metal-centered self-exchange rates in metalloporphyrin polymer films on electrode surfaces,[39] an anomalously large value also is obtained in comparison with $(k_s^{app})_{measd}$. Similarly large discrepancies between heterogeneous and homogeneous charge-transfer rates have been observed for bacteriochlorophylls and bacteriopheophytins.[40] However, comparisons based on low molecular weight aromatic neutral/radical anion couples using double-layer-corrected electrochemical data exhibit a much smaller difference ($k_{ex}^{homo} \sim 10^8$ M^{-1} s^{-1}; $(k_s^{app})_{measd} = 5$ cm s^{-1}; $(k_s^{app})_{calcd} = 3 \times 10^2$ cm s^{-1}).[41] Our data have not been corrected for double-layer effects and we remain cautious about interpretations based on the contents of Table V until such corrections can be made. However, our result is significant in its parallel with recent observations[39,40] of anomalously low values of $(k_s^{app})_{measd}$ for large biologically important molecules. If

(32) This value is the frequency of the Fe–N vibration in Fe(octaethylporphyrin)Cl,[33a] which is deemed to be a valid approximation because M–N vibrational frequencies of high-spin metalloporphyrins are relatively insensitive to M and to porphyrin substituent groups.[33b]

(33) (a) Ogoshi, H.; Watanabe, E.; Yoshida, Z.; Kincaid, J.; Nakamoto, K. *J. Am. Chem. Soc.* **1973**, *95*, 2845. (b) Nakamoto, K. *Infrared and Raman Spectra of Inorganic and Coordination Compounds*; Wiley: New York, 1986; pp 213–221.

(34) Dixon, D. W.; Barbush, M.; Shirazi, A. *J. Am. Chem. Soc.* **1984**, *106*, 4638.

(35) Individual metalloporphyrin redox couples and self-exchange rate constants (M^{-1} s^{-1}): $[Fe(TPPS)(H_2O)]^{3-/4-}$, 1×10^3;[36a] $[Fe(PPIX)(H_2O)]^{0/-}$, 7×10^5;[36b] $[Fe(TMpyP)(H_2O)]^{5+/4+}$, 1.2×10^6;[36c] $[Fe(TMpyP)(Im)_2]^{5+/4+}$, $>1 \times 10^7$;[36c] $[Fe(TMpyP)(H_2O)(OH)]^{4+/3+}$, $>1 \times 10^9$;[36c] $[Fe(PPIX)(CN)_2]^{3-/4-}$, 8×10^{10};[36b] $[Fe(TPP)(1\text{-}MeIm)_2]^{+/0}$, 8×10^7.[34] Abbreviations: TPPS = tetrakis(*p*-sulfonatophenyl)porphyrin; TMpyP = tetrakis(*N*-methylpyridinium-4-yl)porphyrin; PPIX = protoporphyrin IX.

(36) (a) Chapman, R. D.; Fleischer, E. B. *J. Am. Chem. Soc.* **1982**, *104*, 1575. (b) Worthington, P.; Hambright, P. *J. Inorg. Nucl. Chem.* **1980**, *42*, 1651. (c) Pasternack, R. F.; Spiro, E. G. *J. Am. Chem. Soc.* **1978**, *100*, 968.

(37) Heterogeneous rate constants have been reported for ring-centered charge-transfer reactions of both free and metalated porphyrins.[5b,c,7,9] Consistent with the expectation that these reactions are accompanied by little structural change, they exhibit rate constants of the same order of magnitude ($k_s^{app} = 0.01$–0.1 cm s^{-1}) as low-spin metal-centered reductions.

(38) Hupp, J. T.; Weaver, M. J. *J. Phys. Chem.* **1985**, *89*, 2795.

(39) White, B. A.; Murray, R. W. *J. Am. Chem. Soc.* **1987**, *109*, 2576.

(40) Cotton, T. M.; Heald, R. L. *J. Phys. Chem.* **1987**, *91*, 3891.

(41) Kojima, H.; Bard, A. J. *J. Am. Chem. Soc.* **1975**, *97*, 6317.

double-layer corrections are not the sole explanation of the observed difference, then it is likely that solvation energy effects ($\Delta G^{\ddagger}_{os}$) or nonadiabatic factors (A) peculiar to these large molecules are responsible for their low electrochemical rate constants.

Acknowledgment. Support of this research by the National Science Foundation (Grant CHE-84-09594) is gratefully acknowledged. We thank Professor T. M. Cotton for a copy of ref 40 prior to publication.

Registry No. Fe(TPP)OPh, 76282-28-5; Fe(TPP)Br, 25482-27-3; Fe(TPP)Cl, 16456-81-8; Fe(TPP)F, 55428-47-2; Fe(TPP)OAc, 33393-26-9; Fe(TPP)OMe, 29189-59-1; Mn(TPP)Cl, 32195-55-4; Fe(TPP)ClO_4, 57715-43-2; Fe(TPP)$(py)_2^+$, 60542-64-5; Fe(TPP)$(Im)_2^+$, 52155-41-6; Fe(TPP)$(CN)_2^-$, 40988-77-0.

Contribution from the Department of Chemistry, Brown University, Providence, Rhode Island 02912

Kinetic Study of Halide Ionization from Cobalt(III) Porphyrin Complexes. Rate Enhancements Produced by Hydrogen Bonding to the Halide and by Steric Congestion from Coordinated 2-Substituted Imidazoles

Ashfaq Mahmood, Hsiang-lan Liu,[1] John G. Jones,[2] John O. Edwards, and Dwight A. Sweigart*[,3]

Received November 20, 1987

The reaction of Co(TPP)Cl and various imidazoles (RIm) has been investigated in acetone and dichloromethane solvents. Kinetic measurements at room temperature as well as low-temperature spectroscopic, conductivity, and kinetic studies show that Co(TPP)(RIm)Cl is rapidly formed and then slowly converts to $Co(TPP)(RIm)_2^+Cl^-$ in the presence of excess RIm. When the imidazole has a methyl or phenyl group at the N-1 position, the Co(TPP)(RIm)Cl intermediate reacts via rate-determining chloride ionization. With imidazoles bearing a hydrogen at the N-1 position, the chloride ionization is accelerated due to a hydrogen-bonding interaction with the *N*-H group. Although the cobalt porphyrin complexes react much more slowly than analogous iron porphyrins, the two metalloporphyrins follow the same detailed mechanism and display similar sensitivities to hydrogen-bonding interactions. The reaction of Co(TPP)Cl with imidazoles containing a 2-substituent was also studied in order to probe the effect of steric interactions in the intermediate Co(TPP)(RIm)Cl. When a 2-methyl or 2-phenyl substituent is present, the steric strain with the porphyrin ligand increases the lability of the trans chloride by a factor of at least 10; this may be related to "proximal strain" present in certain hemoproteins.

The substitution of cobalt for iron in iron porphyrins and hemoproteins has played an important part in the development of metalloporphyrin chemistry. Cobalt offers several distinct advantages over iron, such as (1) a paramagnetic M(II) state that allows bonding interactions to be probed by ESR and (2) a diamagnetic M(III) state that has a high NMR receptivity. The most important application of these properties has been (1) to probe $M-O_2$ bonding in proteins as well as model systems[4,5] and (2) to probe electronic interactions in cobalt(III) porphyrins via ^{59}Co NMR spectroscopy.[6,7] Of course, the hope is that information gleaned from work with cobalt systems will apply to the iron analogues; this is known to be at least qualitatively true in many cases. However, there are substantial differences between iron and cobalt porphyrins in the thermodynamics and kinetics of axial ligand binding/dissociation, which is related in part to the extra electron on cobalt and the propensity of iron to undergo spin-state changes.

This report concerns hydrogen bonding and steric interactions present in reaction 1, in which X is a halide or pseudohalide and RIm is an imidazole, substituted according to the numbering scheme in structure **2**. The six-coordinate complex Co(Por)-

$$Co(Por)(RIm)X + RIm \rightarrow Co(Por)(RIm)_2^+X^- \quad (1)$$

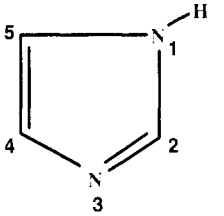

2

(RIm)X (**1**) is susceptible to two types of hydrogen-bonding interactions: from the coordinated (proximal) imidazole *N*-H (if present) to a base and from a proton donor to the coordinated halide. Hydrogen bonding from a proximal imidazole is believed to influence ligand binding, conformational changes, and redox potential regulation in hemoproteins.[8-17] Hydrogen bonding to

(1) Permanent address: Department of Chemistry, Zhejiang University, Hangzhou, Zhejiang, China.
(2) Permanent address: Department of Chemistry, University of Ulster, Coleraine, Northern Ireland BT52 1SA.
(3) Recipient, NIH Research Career Development Award, 1983–1988.
(4) Collman, J. P.; Halpert, T. R.; Suslick, K. S. In *Metal Ion Activation of Dioxygen*; Spiro, T. G., Ed.; Wiley: New York, 1980; Chapter 1.
(5) Brunori, M.; Coletta, M.; Giardina, B. In *Metalloproteins, Part 2: Metal Proteins with Non-redox Roles*; Harrison, P., Ed.; Verlag Chemie: Weinheim, West Germany, 1985; Chapter 6.
(6) Hagen, K. I.; Schwab, C. M.; Edwards, J. O.; Sweigart, D. A. *Inorg. Chem.* **1986**, *25*, 978.
(7) Hagen, K. I.; Schwab, C. M.; Edwards, J. O.; Jones, J. G.; Lawler, R. G.; Sweigart, D. A., submitted for publication in *J. Am. Chem. Soc.*
(8) Walker, F. A.; Lo, M. W.; Ree, M. T. *J. Am. Chem. Soc.* **1976**, *98*, 5552.
(9) Stanford, M. A.; Swartz, J. C.; Phillips, T. E.; Hoffman, B. M. *J. Am. Chem. Soc.* **1980**, *102*, 4492.
(10) O'Brien, P.; Sweigart, D. A. *Inorg. Chem.* **1985**, *24*, 1405.
(11) Poulos, T. L.; Kraut, J. *J. Biol. Chem.* **1980**, *255*, 8199.
(12) Desbois, A.; Mazza, G.; Stetzkowski, F.; Lutz, M. *Biochim. Biophys. Acta* **1984**, *785*, 161.
(13) Stein, P.; Mitchell, M.; Spiro, T. G. *J. Am. Chem. Soc.* **1980**, *102*, 7795.
(14) Shirazi, A.; Barbush, M.; Ghosh, S.; Dixon, D. W. *Inorg. Chem.* **1985**, *24*, 2495.

0020-1669/88/1327-2149$01.50/0